Contrib. Plasma Phys. **52**, No. 5-6, 500 – 504 (2012) / **DOI** 10.1002/ctpp.201210039

Development and Benchmarking of a New Kinetic Code for Plasma Periphery (KIPP)

A.V. Chankin[1]*, **D.P. Coster**[1]**, and **G. Meisl**[1,2]***

[1] Max-Planck-Institute for Plasma Physics, Boltzmannstr. 2, 85748 Garching, Germany
[2] Physics Department, Munich Technical University, 85748 Garching, Germany

Received 08 September 2011, accepted 22 February 2012
Published online 25 June 2012

Key words Kinetic, SOL, Fokker-Planck.

A new kinetic code is presently being developed at IPP Garching to describe parallel (along magnetic field lines) plasma transport in the SOL and divertor of tokamaks. The development of the code is aimed at replacing parallel transport equations used in the present day fluid codes such as SOLPS(B2), EDGE2D, UEDGE. The code is based on the continuum discretisation scheme for the Fokker-Planck equation for parallel plasma transport. In the physical space (along B-lines) the fine spatial structure on the scale of the Debye length is not resolved, instead, plasma quasi-neutrality on a much longer scale, controlled by the parallel electron momentum balance equation, is assumed. At the interface with a material surface, the logical sheath condition is used. The code initially is 1D2V, with parallel and gyro-averaged perpendicular velocities being independent velocity variables. In the future, extension of the kinetic treatment on ions, and extension of the code dimensionality to 2D2V to cover also radial (across magnetic field lines) dimension is envisaged. Details of the code, together with its benchmarking by comparing code results with analytical theory in the limit of highly collisional plasmas, are presented in the paper.

1 Introduction

For typical conditions in the edge regions of magnetic confinement fusion devices plasma collisionality is insufficient to justify the use of fluid codes. This prompted the development of a large number of kinetic codes. The latter differ by: their dimensionality (usually denoted as nDmV, with n being the number of dimensions in the physical space, and m in velocity space), the use of particle-in-cell (PiC) or continuum equations, the use of full-f of delta-δ approximations (especially important for gyro-kinetic codes), spatial resolution for purposes of simulating plasma turbulence (where appropriate), models for the Coulomb collision operator, etc. Review papers [1,2] cover most important features of almost all widely known kinetic codes used for the edge modelling, perhaps, with the exception of the recently developed 2D2V gyro-kinetic code COGENT [3-5]. The closest counterpart of KIPP is kinetic code ALLA (see [6] and refs. therein), with which KIPP shares a number of common features. KIPP development is aimed at integrating kinetic features of parallel plasma transport with the state of the art treatment of neutrals by the Monte Carlo solver EIRENE within the framework of SOL Plasma Simulation code SOLPS (B2.*-EIRENE) [7-9]. At the present earlier stage of the code development, only electrons are treated kinetically, with the ion background specified separately.

All equations of KIPP are written in dimensionless variables, normalised to some physical parameters such as reference electron temperature T_o (and velocity $v_o = \sqrt{T_o/m_e}$), density n_o, and time unit $\tau_o = \frac{v_o^3 m_e^2}{4e^4 n_o \Gamma_o}$, taken to be Trubnikovs basic relaxation time for e-e collisions ([10], p.174), etc., defined by:

$$\tilde{v}_\parallel = \frac{v_\parallel}{v_o}, \quad \tilde{v}_\perp = \frac{v_\perp}{v_o}, \quad \tilde{t} = \frac{t}{t_o}, \quad \tilde{T}_e = \frac{T_e}{T_o} \quad \tilde{n} = \frac{n}{n_o}, \quad \tilde{E}_\parallel = \frac{E_\parallel}{E_o}, \quad \tilde{f}_e = f_e \frac{v_o^3}{n_o}, \quad \tilde{s}_\parallel = \frac{s_\parallel}{s_o} \tag{1}$$

* Corresponding author. E-mail: avc@ipp.mpg.de, Phone: +0049 89 32991844, Fax: +0049 89 32992508
** E-mail: dpc@ipp.mpg.de, Phone: +0049 89 32991865, Fax: +0049 89 32992508
*** E-mail: gmaisl@ipp.mpg.de

where the reference electric field $E_o = |\frac{m_e v_o}{q_e \tau_o}|$, the distance $s_o = v_o \tau_o$, and f_e is the electron distribution function. The Coulomb logarithm $\tilde{\Lambda} = \Lambda/\Lambda_o$ is also dimensionalised, with Λ_o calculated for the reference plasma parameters. In dimensionless parameters, the Fokker-Planck (F-P) equation looks similar to its usual form:

$$\frac{\partial \tilde{f}_e}{\partial \tilde{t}} + \tilde{v}_\parallel \frac{\partial \tilde{f}_e}{\partial \tilde{s}_\parallel} - \tilde{E}_\parallel \frac{\partial \tilde{f}_e}{\partial \tilde{v}_\parallel} = \tilde{C}(\tilde{f}_e) \tag{2}$$

with the dimensionless collision operator on the right hand side. The minus sign before $\tilde{E}$ reflects negative electric charge of electrons. The collision operator in KIPP is the sum of the linear operator for e-i collisions and the non-linear operator for e-e collisions. From now on all expressions will be given in dimensionless parameters (without the tilde sign, $\sim$).

2 Numerical implementation

For the collision operator, equations of Xiong et al. [11] were taken as a starting point and dimensionalised according to the above scheme. For collisions between electrons and particle species β (presently, only electrons and deuterium ion species are included) one obtains:

$$C(f_e, f_\beta) = -\sum_{\beta=e,i} \left(\frac{\partial \Gamma^\beta_{v_\parallel}}{\partial v_\parallel} + \frac{1}{v_\perp} \frac{\partial \Gamma^\beta_{v_\perp}}{\partial v_\perp} \right), \qquad \Gamma^\beta_{v_k} = -D^\beta_{v_k} f_e - D^\beta_{v_k v_\parallel} \frac{\partial f_e}{\partial v_\parallel} - D^\beta_{v_k v_\perp} \frac{\partial f_e}{\partial v_\perp} \tag{3}$$

where v_k refers to $v_\parallel$ or $v_\perp$, and the coefficients D_v and D_{vv} for the background species β are derived from the Trubnikov-Rosenbluth potentials h^β and g^β (converted to our dimensionless variables):

$$D^\beta_{v_\parallel} = 4\pi\Lambda n \frac{m_e}{m_\beta} \frac{\partial h^\beta}{\partial v_\parallel}, \qquad D^\beta_{v_\parallel v_\parallel} = -4\pi\Lambda n \frac{\partial^2 g^\beta}{\partial v_\parallel^2}, \qquad D^\beta_{v_\parallel v_\perp} = -4\pi\Lambda n \frac{\partial^2 g^\beta}{\partial v_\parallel \partial v_\perp}$$

$$D^\beta_{v_\perp} = 4\pi\Lambda n \frac{m_e}{m_\beta} v_\perp \frac{\partial h^\beta}{\partial v_\perp}, \qquad D^\beta_{v_\perp v_\perp} = -4\pi\Lambda n v_\perp \frac{\partial^2 g^\beta}{\partial v_\perp^2}, \qquad D^\beta_{v_\perp v_\parallel} = -4\pi\Lambda n v_\perp \frac{\partial^2 g^\beta}{\partial v_\perp \partial v_\parallel} \tag{4}$$

Potentials h^β and g^β are dimensionless variants of expressions given by Hinton [12] for the case of a cylindrical geometry ($v_\perp$ incorporates two degrees of freedom):

$$h^\beta = -\frac{1}{4\pi} \int \frac{f_\beta(\vec{v}')}{\mid \vec{v} - \vec{v}' \mid} d\vec{v}' = -\frac{1}{\pi} \int_0^\infty v'_\perp dv'_\perp \int_{-\infty}^\infty \frac{K(k)}{u} \frac{f_\beta(v'_\parallel, v'_\perp)}{n} dv'_\parallel,$$

$$g^\beta = -\frac{1}{8\pi} \int \mid \vec{v} - \vec{v}' \mid f_\beta(\vec{v}') d\vec{v}' = -\frac{1}{2\pi} \int_0^\infty v'_\perp dv'_\perp \int_{-\infty}^\infty \frac{E(k)}{u} \frac{f_\beta(v'_\parallel, v'_\perp)}{n} dv'_\parallel, \tag{5}$$

where K and E are complete elliptic integrals, $u = \sqrt{(v_\perp + v'_\perp)^2 + (v_\parallel v'_\parallel)^2}$, $k = 2\sqrt{v_\perp v'_\perp}/u$. For inner points of the velocity grid, potentials h^β and g^β can also be calculated by solving the two Poisson equations:

$$\Delta_v g^\beta = h^\beta, \qquad \Delta_v h^\beta = f^\beta / n \tag{6}$$

with the Laplacian in cylindrical coordinates.

For the linear (e-i) collision operator, with fi replaced by a Maxwellian, analytical expressions for the Trubnikov-Rosenbluth potentials and D-coefficients figuring in Eq. (4) can be found e.g. in [10]. In KIPP, dimensionless expressions for these coefficients via variable $v_{gi} = v/\sqrt{2T_i/m_i}$ ($v = \sqrt{v_\parallel^2 + v_\perp^2}$), error function $G(x)$ and function $H(x) = G(x) - xG'(x)$ can be found in [13].

The F-P equation (2) is solved by using an operator splitting scheme, with 1/2 of the time step Δt for parallel propagation along $s_\parallel$ (free-streaming) followed by Coulomb collisions plus the electric field force over Δt, followed again by another $1/2\Delta t$ of the free-streaming, as proposed by Shoucri & Gagne in [14] and implemented

also in [6]. A number of $2^{\rm nd}$ order explicit schemes with upwinding were tested for the free-streaming. At the Debye sheath, full reflection of f_e for sub-threshold $v_\parallel$ (with parallel energies below the Debye sheath potential drop) at the spatial cell face bordering the sheath is specified, with zero f_e for faster electrons not returning from the sheath, similar to [6] and ensuring zero current density through the sheath. Plasma quasi-neutrality away from the Debye sheath is maintained by adjusting $E_\parallel$ to compensate for parallel momentum generation in each spatial cell. This is a numerical procedure not requiring any equations. Contributions to the momentum generation are expected from the free-streaming and e-i thermoforce. The effect of the former can be easily calculated from the electron pressure gradient and subtracted from the code-calculated momentum generation. The result can be compared with analytical expressions for the thermoforce.

In velocity space, a rectangular mesh (unlike spherical coordinate mesh of [6]) is used, similar to the 1D2V kinetic code fp [15]. This allowes a straightforward implementation of boundary conditions at the Debye sheath, where fe undergoes a sharp cut-off in $v_\parallel$ owing to the logical sheath boundary condition used. No attempts were made to implement and test spherical velocity coordinates. However, in the tests involving spherically symmetric problems (e.g. e-i energy equipartition, see below), deviations of f_e from a Maxwellian showed very high degree of spherical symmetry. For an adequate coverage of a wide range of T_e's along the field line, a slightly non-uniform grid can be used, with the velocity cell size increasing by the parameter EPS=$1+\varepsilon(\varepsilon << 1)$ from cell to cell in both parallel and perpendicular directions. The number of velocity cells is controlled by the parameter $mmax$, with ($mmax$+1) cells for $v_\perp$ and (2$*mmax$+1) – for $v_\parallel$. The maximum velocity is given by $vparmax$ (typically 10; remember that all values are now given in dimensionless units, so 10 for velocity implies 10 v_o, time is measured in τ_o, space in $s_o = v_o\tau_o$, etc.).

A fully implicit scheme (with an option to switch between the Euler and Crank-Nicolson schemes) for solving the F-P equation (2) in velocity space (0d2v problem, spatial dimension ignored) is used, based on the finite volume 9-point (3×3) stencil discretisation, with particle conservation achieved by specifying fluxes between cells. The $1^{\rm st}$ order implicit upwind scheme for the description of the $E_\parallel$-field force effects in velocity space, requiring the 3-point stencil, can be easily blended into the 9-point implicit scheme for the collision operator, to describe the combined effect of Coulomb collisions and the $E_\parallel$-field force. Tests showed that the combined scheme, despite being only $1^{\rm st}$ order accurate to describe the $E_\parallel$-field force effects in velocity space, performed as a $2^{\rm nd}$ order scheme for velocity grids used, indicating that the $E_\parallel$-field force is sub-dominant for slightly non-uniform grids used (see below). All fluxes through cell faces at grid boundaries are set to zero, except for those allowing leakage caused by the $E_\parallel$-field force in the direction outside of the grid. To calculate Trubnikov-Rosenbluth potentials, Poisson Eqs. (6) were solved in sequence using the 5-point stencil discretisation scheme, with h^β and g^β (where $\beta \equiv e$ presently) at the grid boundaries calculated according to (5). At each time step, the sparse matrix solver MUMPS [16] is called 3 times: to solve sequentially two Poisson equations and one $F-P$ equation.

3 Performance tests

All tests performed so far for the KIPP validation and benchmarking delivered good results: tests on stability of numerical schemes for all parts of the code, relaxation to a (drifting) Maxwellian by Coulomb collisions, etc. Momentum and energy are however not conserved by our non-linear e-e collision operator. The energy downward drift $\propto mmax^{-2}$, being $\sim 0.01\%$ for $\Delta t = 1$ (of τ_o, in real time units) and $mmax \approx 200$, and scales linearly with the time step. It is compensated by adding power to $v_\perp$ component of f_e. The momentum non-conservation is several orders of magnitude smaller and is neglected. Some of the tests aimed at benchmarking against classical expressions for transport coefficients in the limit of high plasma collisionality are described below.

3.1 Electrical conductivity

An implicit scheme for the combined effect of Coulomb collisions and the $E_\parallel$-field force produced saturated electric currents after $t \sim 130$ (in dimensionless time units) for $E_\parallel$-fields << Dreicer's. Electric current is converted into the dimensionless electron velocity assuming non-moving ions: $v_\parallel = KT_e^{3/2}E_\parallel/n\Lambda$. The most precise analytic result was given by Kaneko et al. [17]: K = 7.425886. Fig. 1 shows how the relative deviation of KIPP results from Kaneko's is reduced to negligible values by the velocity grid refinement. Calculations were

done on a uniform grid with $vparmax = 10$. Non-uniform grids used, with EPS = 1.01-1.05, produced similar quality matches, all manifesting 2nd order convergences.

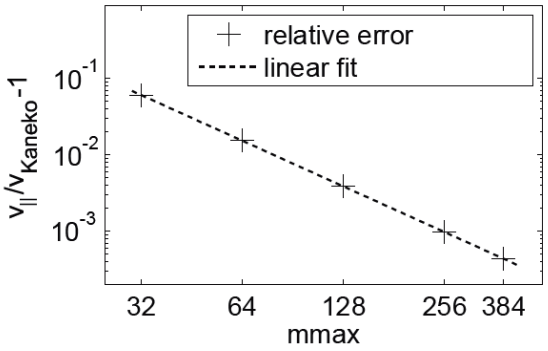

Fig. 1 Convergence of KIPP results to Kaneko's after t=130(τ_o).

3.2 Electron-ion energy equipartition

For initially Maxwellian $f_{e,i}$, equipartition rate between electrons and deuterium ions agrees well with Trubnikov's result ([2], Eq. (20.3)) for small time steps, see Fig. 2a for a uniform grid with $mmax = 200$, $vparmax = 10$. The larger disagreement around $T_i \sim T_e$ is attributed to smallness of the denominator, resulting in an amplification of numerical errors.

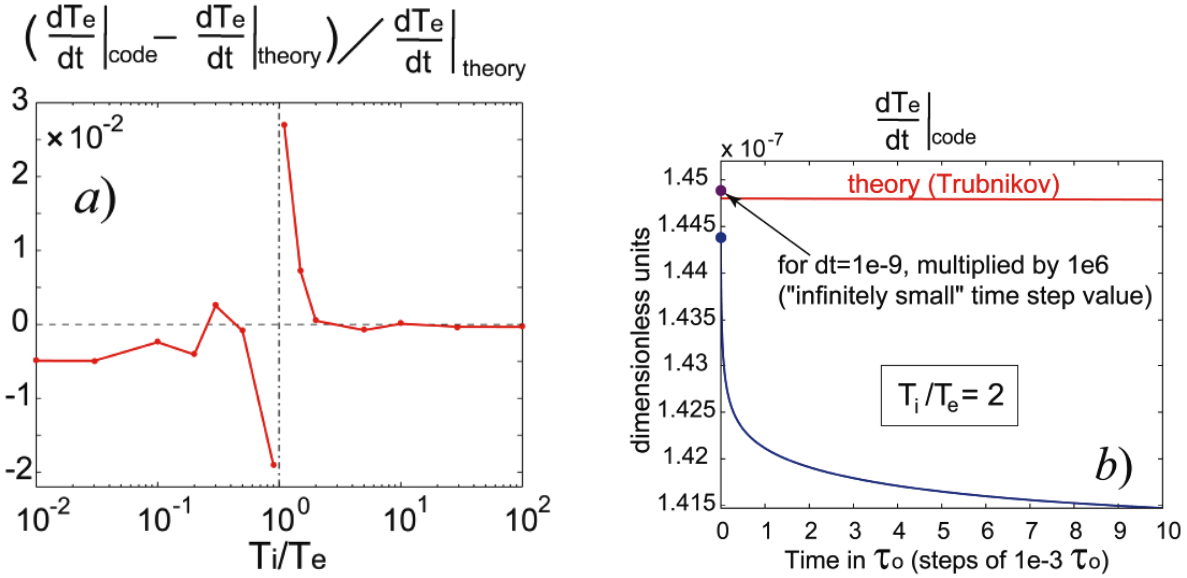

Fig. 2 Convergence of KIPP results with theoretical rate for $e - i$ (with $i \equiv D^+$) energy equipartition rates.

For larger time steps and/or longer run times, deviations from theory occur (Fig. 2b), due mostly to the f_e deviation from a Maxwellian, for $T_i \neq T_e$. This subtle effect of Coulomb collisions is attributable to slowest test electrons with energies $< 1/390 \times T_i$ (for deuterium ions) gaining energy from ions at very high collision rates, with the majority of (more energetic) electrons losing their energy to the ions at much lower rates (see Eq. (20.1) of [10] and surrounding text). KIPP results for the deviation from theory [10] (which assumes Maxwellian $f_{e,i}$ distributions) for various T_i/T_e and m_e/m_i ratios are in a broad agreement with an earlier study of Bobylev et al. [18]. For a Maxwellian $f_{e,i}$ and $T_i = T_e$, f_e profile effects compensate for test electron energy gains/losses, resulting in a full thermodynamic equilibrium. We also independently confirmed Trubnikov's test particle equation (20.1), by deriving it starting from our set of Eqs. (3-4) with simplified D-coefficients corresponding to

a Maxwellian background [13] (i.e. for the case of a linear collision operator), and by assuming fe to be a delta-function in velocity space.

3.3 Electron parallel heat conduction and electron-ion thermoforce

Both coefficients were found to be in agreement with Braginskii's formulas [19] within a few % in a dedicated series of long runs with small time steps ($\Delta t < 0.5$, of τ_o, in real time), long system lengths ($s_{\|} = 1000$; i.e. 1000 of $\tau_o v_o$ - collision mean free paths in real space units) and small ($\sim 10\%$) T_e drops between the power input point and the Debye sheath.

4 Performance tests

KIPP is parallelised under MPI and is run on 64 processors of the Linux cluster. Coulomb collisions are computed simultaneously by 63 processors, each dedicated to a different spatial position. On a velocity grid with $mmax = 200$ one time step takes ~ 3 s in real time.

Acknowledgements Discussions with Drs. A. Bergmann, R. Bilato, H.-J. Klingshirn, Prof. K. Lackner, and Dr. G. Pereverzev are acknowledged.

References

[1] W. Fundamenski, Plasma Phys. Control. Fusion **47**, R163 (2005).
[2] R.H. Cohen and X.Q. Xu, Contrib. Plasma Phys. **48**, 212 (2008).
[3] M.R. Dorr et al., in : Proceedings of the SciDAC 2010 Conference, Tennessee, USA, http://computing.ornl.gov/workshops/scidac2010/papers/math_m_dorr.pdf
[4] T.D .Rognlien et al., 2010 Proc. 23rd IAEA Conf. on Fusion Energy (Dajon, Rep. of Korea, October 2010), http://www-pub.iaea.org/mtcd/meetings/PDFplus/2010/cn180/cn180_papers/thd_p3-05.pdf
[5] M.A. Dorf et al., "Progress with the COGENT Edge Kinetic Code: Collision Operator Options", paper P1-14, this Workshop.
[6] O.V. Batishchev et al., J. Plasma Physics **61**, 347 (1999).
[7] R. Schneider et al., J. Nucl. Mater. **196198**, 810 (1992).
[8] D. Reiter, J. Nucl. Mater. **196198**, 80 (1992).
[9] D.P. Coster et al., Proc. 18th IAEA Conf. on Fusion Energy (Sorrento, Italy, October 2000) CD-ROM paper IAEA-CN-77/EXP5/32 (Vienna: IAEA) (2000).
[10] B.A. Trubnikov, "Particle interaction in a fully ionized plasma", Review of Plasma Physics Vol. 1, A.M.Leontovich (ed.), Consultants Bureau, New York 1965.
[11] Z. Xiong, R.H. Cohen, T.D. Rognlien, and X.Q. Xu, Journal of Computational Physics **227**, 7192-7205 (2008).
[12] F. Hinton, "Simulating Coulomb Collisions in Particle Codes", TCC remote seminar 2007, http://fusion.gat.com/THEORY/images/c/ca/Hinton05082007.pdf.
[13] G. Meisl, "Study of kinetic phenomena in homogeneous plasmas using the new Fokker-Planck code KIPP", diploma work, IPP Garching (2011).
[14] M.M. Shoucri and G. Gagne, J. Comput. Phys. **27**, 315 (1978).
[15] D.P. Coster, Ph.D. Thesis, Princeton Plasma Physics Laboratory, Princeton, USA (1993), http://www.ipp.mpg.de/dpc/thesis_single.pdf
[16] P.R. Amestoy, I.S. Duff, J. Koster and J.-Y. LExcellent, "A fully asynchronous multifrontal solver using distributed dynamic scheduling", SIAM Journal of Matrix Analysis and Applications **23**, 15-41 (2001).
[17] S. Kaneko and M. Taguchi, J. Phys. Soc. Jpn. **45**, 1380 (1978).
[18] A.V. Bobylev, I.F. Potapenko, and P.H. Sakanaka, Phys. Rev. E **56**, 2081 (1997).
[19] S.I. Braginskii, "Transport processes in a plasma", Review of Plasma Physics Vol. 1, A.M. Leontovich (ed.) Consultants Bureau, New York (1965).

